Algerian Journal of Environmental Science and Technology
June edition. Vol. 9. N°2. (2023)
ISSN : 2437-1114
www.aljest.org

Analysis and NOx prediction in turbulent non-premixed swirling flame

D. Lalmi[1], A. Bellaouar[1*], A. Benali[1,2], R. Hadef[3]

[1]Laboratory of Materials, Energy Systems Technology and environment "MESTEL", Faculty of sciences and technology, Université de Ghardaia. 47000, Ghardaïa. Algeria
[2]Department of mechanical, University A.T. of Laghouat, Laghouat, Algeria
[3]Faculty of sciences and applied sciences, University of L'Arbi Ben M'hidi, Oum el Bouaghi, Algeria

*Corresponding author: mestel@univ-ghardaia.dz

ARTICLE INFO

Article History:

Received ***: 27/11/2020***
Accepted ***: 24/07/2021***

***Key Words*:**

Swirl;
Flame;
Simulation;
Turbulence;
Nnitride oxide and pollution.

ABSTRACT /RESUME

Abstract: *In this paper, a numerical investigation of the of methane air mixture combustion by using the ansys flut in its version 16.0 is presented . The aim objective is to predicte the NOx emissions in the combustion of a swirling turbulent flame . In this study various parameters like proprieties of turbulent swirling flame and the status of the research on NOX formation /reduction are discussed. the combustion model used is the PDF Flamelet Model for non premixed gas combustion. The obtained results of this work will help in finding out the geometry of the combustion chamber which will lead to less emission of NOx .*

I. Introduction

In recent years, the role of combustion technology in human life has been highlighted because over 90% of worldwide energy demand has been satisfied using combustion methods [1]. The augmentations in combustion efficiency and pollutant reduction have become the main concerns of combustion researchers in academic societies and of industrial manufacturers[2]. In the combustion process, a reaction between the fuel and the oxidizer occurs to release heat (thermal energy) and consequently generate electricity. Numerous emissions, such as unburned hydrocarbon, carbon dioxide (CO2), carbon monoxide (CO), nitride oxide (NOX), soot, and particulate matter, are often released into the atmosphere during combustion[3].

These undesirable pollutants can jeopardize the environment as the rate of their production increases because of rapid industrialization[4]. Thus, new combustion methods have been introduced to overcome the environmental dilemmas in combustion[5]. For instance, lean premixed combustion technology was investigated to suppress combustion product temperature and, consequently, low pollutant formation[6]. However, flashback and poor combustion stability were mentioned as the main disadvantages of this method[7-8]. Flameless combustion technology was recently introduced as a promising technique for concomitantly reducing pollutant formation and fuel consumption[9-11]. This sophisticated combustion method has been given various names because of its varied characteristics.

This sophisticated combustion method has been given various names because of its varied characteristics. To achieve this requirement the burner design is commonly based on the common injection of air and gaseous fuel in the form of swirling flow. It results in an enough adverse pressure along the axis, forming a swirl-induced central toroidal recirculation zone (CTRZ) which is only formed beyond a critical value of the swirl number, around 0.5~0.6 [12]. Once the CTRZ is established, it anchors the flame, thus improving the flame stabilization by returning hot gases and active radicals back to the jet core leading to a more stirred mixture.

Most modern gas turbines use double-concentric swirl-burner because it gives the freedom to vary the distribution of axial and angular momentum of different airflow and mixing patterns can be achieved, resulting in substantial reduction in NOx emissions and lean blow off (LBO) limit in comparison to single swirler burner[13]. This technology is attractive to fit producing the required power in small size and compact combustor because several ignitions are distributed at the combustor head without any side wall among igniters. So, the more detail understanding of the dynamic flow and mixing in this annular combustor is very important to improve engine power and efficiency. Such reasons are closely related to the motivation of this study.

On the other hand, the fast development of computer and methodology of numerical computation technology have enabled computational fluid dynamics (CFD) to play a great role in designing combustors design because of its low cost compared with experimental testing. CFD is very effective when used as a guide for potential experimental investigations, particularly when experimental data is available for at least one test condition, for comparison with the CFD predictions. Since the accuracy of mixing predictions for these flows plays a crucial role in the simulation of gas turbine combustion, a number of CFD studies were carried out to get information on the swirling flow field inside the combustor but prediction of such a flow pattern pose a daunting challenge since the developed recalculating flow pattern is the result of a multitude of complex processes involving strong shear regions, high turbulence, very large curvature of streamlines within the flow and rapid mixing rates. In this paper, the roprieties of turbulent swirling flame in combustion chamber and the status of the research on NOX formation /reduction in are discussed .

II. Materials and methods

II.1. Mathematical formulations

The balance equations governing the reacting flow are: mass, momentum, species and energy. The founder idea of large eddy simulation (LES) is to resolve the large turbulent motions in a flow field and to modeling only the effects of small ones. The resolved contribution $\bar{f}$ is obtained by applying the spatial LES filter to instantaneous variables f. Filtering the instantaneous governing equations and introducing the Favre filtered variables $\tilde{f} = \overline{f\rho}/\bar{\rho}$ [12-14].

$$\frac{\partial \bar{\rho}}{\partial t} + \nabla \cdot \left(\bar{\rho}\tilde{u}_i\right) = 0 \qquad \textbf{(1)}$$

Momentum quantity conservation equation:

$$\frac{\partial}{\partial x_l}(\bar{\rho}\tilde{u}_i\tilde{u}_l) = -\frac{\partial \bar{P}}{\partial x_i} + \frac{\partial}{\partial x_l}\left(\bar{\tau}_{il} - \bar{\rho}(\widetilde{u'_i u'_l} - \tilde{u}_i\tilde{u}_l)\right) \qquad \textbf{(2)}$$

Chemical species conservation equation:

$$\frac{\partial}{\partial t}(\bar{\rho}\tilde{Y}_k) + \frac{\partial}{\partial x_i}(\bar{\rho}\tilde{u}_i\tilde{Y}_k) = \frac{\partial}{\partial x_i}\left(\rho D_k \frac{\partial \tilde{Y}_k}{\partial x_i} - \bar{\rho}(\widetilde{u_i Y_k} - \tilde{u}_i\tilde{Y}_k)\right) + \dot{\omega}_k;\ldots\ldots k = 1, N \qquad \textbf{(3)}$$

Energy conservation equation

$$\frac{\partial}{\partial t}(\bar{\rho}\tilde{h}_s) + \frac{\partial}{\partial x_i}(\bar{\rho}\tilde{u}_i\tilde{h}_{sk}) = \frac{\partial \bar{p}}{\partial t} + \tilde{u}_i\frac{\partial \bar{p}}{\partial x_i} + \frac{\partial}{\partial x_i}\left(\lambda\frac{\partial \tilde{T}}{\partial x_i} - \bar{\rho}(\widetilde{u_i h_s} - \tilde{u}_i\tilde{h}_s)\right) - \sum_{k=1}^{N}\dot{\omega}_k\Delta h^0_{f,k} \qquad \textbf{(4)}$$

Gas state equation:

$$\bar{P} = \bar{\rho}\tilde{r}\tilde{T} \qquad \textbf{(5)}$$

where: Ui and u'i are the components average and fluctuating velocity in the direction xi, Yk is the methane mass fraction, P is the pressure, μ is the dynamic viscosity and ρ is the density of the fluid. The hs is the sensible enthalpy, λ is the thermal conductivity; Dk is the species diffusivity; Is estimate to the ratio of kinematic viscosity to Schmidt number ScK which is assumed to be 0.7 in this study; T is the temperature; $\dot{\omega}_k$ is the secrecies reaction rate and the $\Delta h^0_{f,k}$ is the formation enthalpies of species. Fick's law in the Equ (3) describes the mass flux.

The viscous heating term and radiation term in Equ (4) are neglected as they are negligible compared to the combustion source term. $\bar{\tau}_{il}$ Is the stress tensor and the deviatoric part of filtered strain tensor is defining us:

$$\tilde{S}_{ij} = \left(\frac{1}{2}\right)\left(\left(\frac{\partial \tilde{u}_i}{\partial \tilde{x}_j}\right) + \left(\frac{\partial \tilde{u}_j}{\partial \tilde{x}_i}\right)\right) \qquad \textbf{(6)}$$

In this calculating method of turbulent flows offers a good compromise between computational cost and adequate description of unsteady turbulence. The LES equations are obtained by filtering the Navier-Stokes equations at the scale l. In a calculation code LES; the filtering operation is carried out implicitly by the mesh and the numerical scheme: the structures of the turbulence smaller than l are not solved by the calculation but taken into account by the LES model. The dissipation and dispersion errors of the numerical scheme contribute to the increase of the filter size.

For more detailed concerning LES approach, we refer to [15].

II.2. Experimental Test Case

When The Adopted configuration has been investigated experimentally [16], through laser Doppler anemometry (LDA). It consists of two co-swirling airflows injected through a central nozzle (diameter 15 mm) and an annular nozzle (i.d. 17 mm, o.d. 25 mm widening to 30 mm at the exit). Non-swirling gaseous fuel (CH_4) is injected through an annular slit between both airflows, which results in a high degree of premixing before ignition at a few millimeters upstream the burner exit.
The diameter of the combustion chamber is $D_{CC} = 4D_0$ and its length is $D_{CL} = 18D_0$. Limitation of the main reaction zone was provided by an orifice with 70% diameter reduction placed at the exit of the combustion chamber. This outlet geometry avoids back-flow through the exit section, otherwise could be induced by the lowered pressure on the axis of the rotating fluid. The flow is axially accelerated by the constriction at the outlet of the combustion chamber. This helps to turn the flow from a subcritical state after the vortex breakdown to a supercritical flow at the outlet [Escudier and Keller 1985]. Based on these measurements, the sensitivity of the recirculation region to the outlet conditions can be reduced.

The mass flow rates of air and methane were adjusted at $\dot{M}_a = 64\,\text{kg/h}$ and $\dot{M}_f = 1.8\,\text{kg/h}$, corresponding to an air equivalence ratio $\lambda = 2$ and a through-flow time of 180ms $Y_{f,0} = 0.02735562$. The air stream through the nozzle was electrically preheated up to 400°C $\left(\rho = 1.0924 kg/m^3 \mu = 1.95710^{-5} kg/s - m\right)$ and split between the inner circular passage $\left(0.37\dot{M}_a, 23.68 kg/h, 35.80 m/s, \text{Re}_i = 49962\right)$ and the outer annular canal. The global Reynolds number is calculated as the product of the axial average air velocity $(U_0 = 34.83 m/s)$ at the nozzle exit defined as z=0 and the throat diameter of the diffuser divided by the kinematic viscosity of air and gives approximately.The swirl strength is characterized by the outlet swirl number S_0, defined as the ratio of angular to axial momentum flux in the nozzle divided by the outside nozzle radius R_0 as given by:

$$S_0 = \frac{\int_0^{R_0} \rho\left(\overline{U}\,\overline{W}r + \overline{u'w'}r\right) r\,dr}{R_0 \int_0^{R_0} \rho\left(\overline{U}^2 + \overline{u'}^2\right) r\,dr} \quad (7)$$

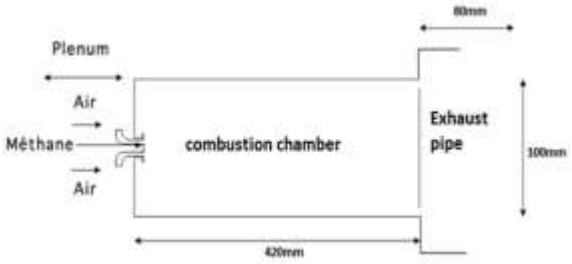

Figure 1. *Sketch of the Geometrical configuration*

The theoretical swirl number S_{th} calculated from only the geometrical data of the swirl generator is used since it is approximately equal to S_0 [21]. It is of the inner airflow $S_{th,in} = 0.46$ and of the outer air flow $S_{th,out} = 1.0$, yielding the overall swirl number is $S_{th,total} = 0.81$. This geometrical configuration is shown on Figure1.For more detailed specifications concerning the combustor; we refer to [17].

II.3. Combustion model

One of the crucial steps to modeling combustion in ansys fluent 16.0 is the choice of combustion model. So we must first choose a Premixed Combustion or Non-Premixed Combustion options. This determines whether or not the reactants present are initially mixed. From this stage, several choices of combustion model are available to us. Here we want to study a turbulent diffusion flame (Non-Premixed Combustion). In this model, it needs to create the PDF table, where all parameters and its information's on thermo-chemistry interactions with turbulence are adopted. All quantities values or all species like as fuel and oxide at the inlet has been induced in their experimental values cited in fourth parts and controlled in the PDF table. The PDF table over view to display temperature and reacting species: methane, oxygen and carbon dioxide with mixture fraction Figure 2 below. We can see that the maximum of temperature is 2200K corresponding to 0.125 of mixture fraction.

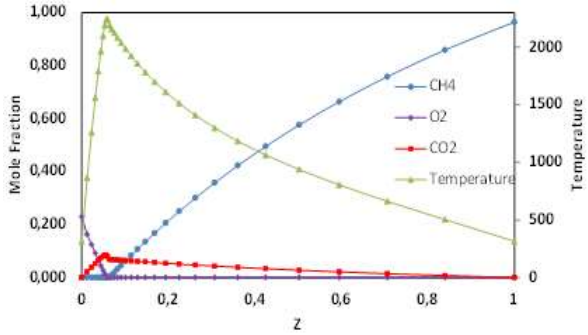

Figure 2.*Temperature and different species evolution with mixture fraction*

II.4. NOx Formation during the combustion process

Nitrogen oxides are considered the most relevant pollutants. The principal nitrogen oxides found in the atmospheric are nitric oxide (NO), nitrogen dioxides (NO_2), which is normally referred to as NOX, and nitrous oxide (N2O)[18-20]. The NOX and N_2O pollutant emissions in the atmosphere have increased since the middle of the last century. Researchers have recently conducted studies to reduce NO and general NO_X emissions in combustion systems. NO is mostly produced within the reaction zone. The eventual oxidation to NO_2 occurs in a post-burn process away from the combustion region [16,13,21]. N_2O is mostly emitted from combustion sources. Four main NO sources are produced in the combustion process: thermal NO or Zeldovich mechanism, prompt NO or Fennimore mechanism, fuel NO, and N_2O. The main features of each NO formation mechanism are discussed in the following section [22].

Thermal NOx

The construction of thermal NO corresponds to the direct oxidation of nitrogen molecules. The three principal reactions of the thermal NO formation mechanism are indicated as follows:

$$N_2 + O \leftrightarrow NO + N \quad \textbf{(8)}$$

$$N + O_2 \leftrightarrow NO + O \quad \textbf{(9)}$$

$$N + OH \leftrightarrow NO + H \quad \textbf{(10)}$$

Thermal NO or Zeldovich mechanism is produced during the combustion process. Equations (3) and (4) show that N_2 and O_2 form the chain propagating steps known as the Zeldovich mechanism. The rate limiting reaction in NO formation is the N_2+O↔NO+N reaction. Thermal NO is strongly dependent on temperatures above 1500 °C. The rate of formation rapidly increases with increasing temperature as a result of high activation energy (approximately Ea = 319 kJ/mol) [23,24].

Prompt NOx

Prompt NO formation, which occurs in fuel-rich systems, is a nitrogen oxide formation method described by Fennimore. Prompt NO can be found in the flame zone and involves a hydrocarbon species and the atmospheric nitrogen N_2. This NO formation mechanism is popularly termed 'prompt' because of the very early appearance of the flame at the flame front. The formation mechanism depends on the mixing rate of fuel and air. The formation of prompt NO follows the following reaction paths [25]:

1-The reactions of N_2 with hydrocarbon fragments produce cyanide (HCN).

$$CH + N_2 \leftrightarrow HCN + N \quad \textbf{(11)}$$

2. Ammonia radicals (NH, NH_2) are generated by HCN hydrogen abstraction reactions with oxy-cyanogens.

$$HCN + O \leftrightarrow NCO + H \quad \textbf{(12)}$$

$$NCO + H \leftrightarrow NH + CO \quad \textbf{(13)}$$

3. Ammonia radicals form NO

$$NH + H \leftrightarrow N + H_2 \quad \textbf{(14)}$$

$$N + OH \leftrightarrow NO + H \quad \textbf{(15)}$$

Fuel NOx

Fuel NO_X commonly originates from nitrogen-bearing fuels, such as certain solid and liquid fuels. Fuel NO_X is formed through the nitrogen oxidation contained in the fuel. Fuel NO_X is created once the nitrogen is chemically bound to the fuel by excess oxygen during combustion. During combustion, the nitrogen bound to the fuel is released as a free radical and ultimately forms free N_2 or NO. The production of fuel NO_X is dependent on the stoichiometric ratio between air and fuel. Fuel-rich mixtures generally result in high NO_X formation, implying that such process is independent of fuel type [26].

The figure 3 show one of the proposed reaction of NO formation at the mechanism.

Algerian Journal of Environmental Science and Technology
June edition. Vol. 9. N°2. (2023)
ISSN : 2437-1114
www.aljest.org

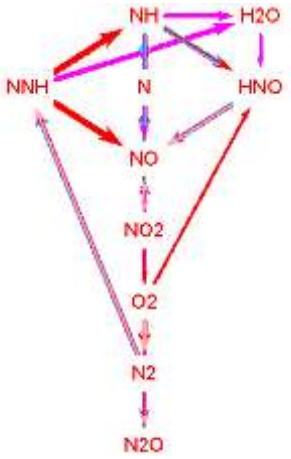

Figure 3. *One of the proposed reaction of NO formation at the mechanism*

Solving method

In this investigation; ANSYS-Fluent 16.0 CFD software has been used in which was intensely validated and compared well with the experience. The solver is based on the finite volume method for resolving all transport equations. Turbulence was modeled by the LES (large eddy simulation) with the WALE subgrid-scale viscosity has been considered. The default scheme time discretisation assumed in this study was the second order. PISO, algorithm procedure was used for coupling the pressure and velocity fields for incompressible flow. By using this solver; the equations show a fast convergence. All equations are resolved numerically in unsteady case using a grid of 0.80 million hexahedral cells with convergence criteria about 10-6. Three types of boundary conditions were applied in this study; Inlet, outlet and wall. At the input of the combustion chamber all values of different parameters are measurements; like the velocities (U, V, W) species and turbulent kinetic energy by a specifically UDF algorithm of profiles type. Except dissipation of turbulent kinetic energy which is calculated by this equation:

$$\varepsilon = C_{\mu}^{0.75} \frac{k^{1.5}}{0.7D} \qquad \textbf{(16)}$$

III. Results and discussion

III.1. Validation

In a first step, a description will be given of the mean structure of the flow. Figure4 show mean axial velocity component at different section in the combustion chamber. The presence of the central recirculation zone CRTZ as well as the zones of the CRZ corners is observed. Comparison is possible with the preceding calculations because the flow rates have been adapted as a function of the temperature of the injected air. For this we can point out some differences between the two configurations: the angle of opening of the flow is more important in the case against swirl. The maximum axial velocities are greater in the case against swirl than in the reactive case, as well as the shape of the recirculation zones are slightly modified and the expansion of the flow is done more regularly in the two cases with a very large opening.

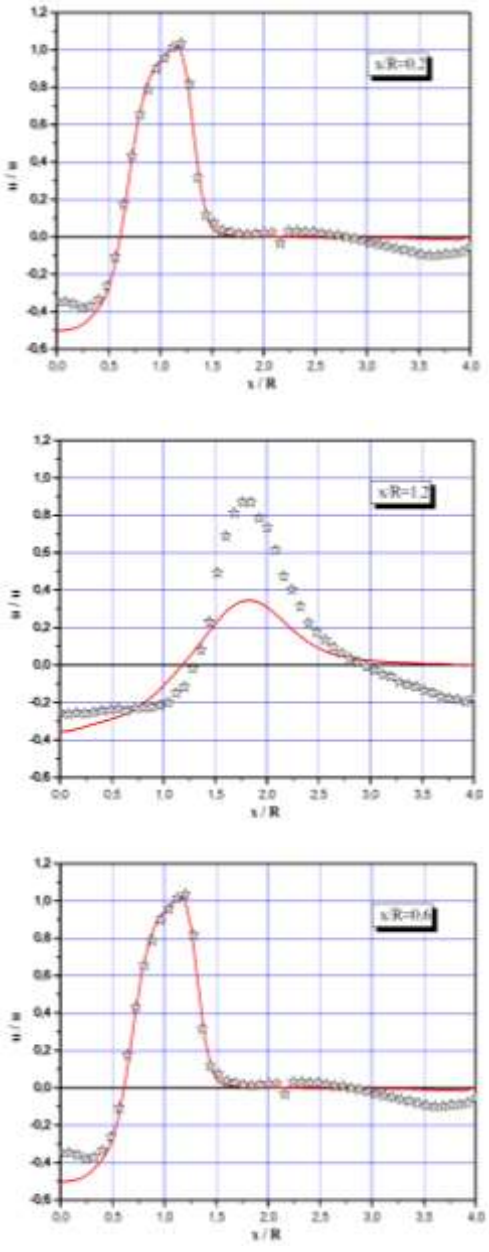

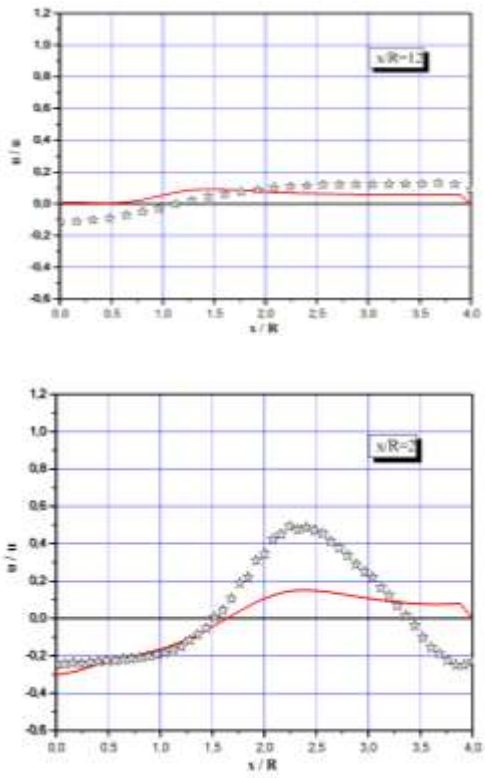

Figure 4.*Validation with experiment of axial velocity at different section*

The peak gas temperature is located in the primary reaction zone where the combustion of mixture of air and methane takes place. The fuel from the injectors is first mixed in the swirling air before burning in the primary reaction zone. The gas temperature decreases after the primary reaction zone due to the dilution of the flame with the secondary air.

Temperature profiles are plotted at different axial position to understand the propagation of combustion flame in chamber. Figure 5 shows the temperature profiles of methane/air combustion in combustion chamber at deferent axial positions of Z = 5 mm, 25 mm, and 55 mm respectively and normalized by the radius of the combustion chamber .

The first profile (Z= 5 mm) represents the gas temperature near the fuel injections. The fuel is injected from the fuel inlets and mixed with the swirling air before the start of the combustion. The size of the flame increases downstream and reaches a maximum at radius Z = 25 mm. Clear flame visualization is observed having maximum temperature of 2300 K. The temperature of the flame decrease after that with the increase of the axial distance (Z=55mm).

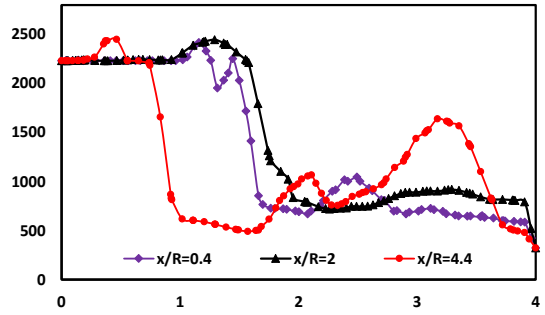

Figure 5. *Temperature profiles evolution at different section in combustion chamber*

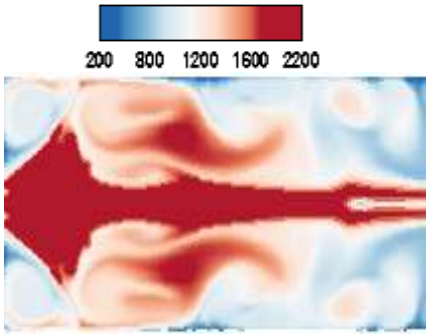

Figure 6. *Temperature evolution at different section in combustion chamber*

Effect of biosorbent dose

The effect of biosorbent dose in the range of 2 to 10 g L^{-1} was used for the adsorption experiments and the results are given in Figure 7. We note that, the removal rate of Ni(II) ions increases gradually with increasing biosorbent dose. It increases from 5.06 to 35.46 %. This raise in removal rate of Ni(II) ions could be due to availability of more surface area and functional groups. The biosorbent dose of 10 g L^{-1} is considered as equilibrium value and was taken as the optimal biosorbent dose for the subsequent experiments.

The mass consumption of the methane represented in radial profiles form of at different axial positions in combustion chamber. The consumption of the fuel is clearly illustrated, because the mass fraction of methane decreases from the initial value at the outlet of the jet and totally burned just on front flame to give the carbon dioxide and the water vapor. It is noted that the excess of air is translated by an excess of oxygen which remains in the products of the combustion .Among the species produced, the mass fraction of Co_2 is also expressed as radial profiles in different positions (x / R=5 ,25and 55). it can be sayed fo the description of the behavior of this parameter ; by crossing the front flame, the mass fraction is increased to reach maximum values. Downstream of the front of the flame, the concentration of these species decreases since they mix with the air of the surrounding.

Algerian Journal of Environmental Science and Technology
June edition. Vol. 9. N°2. (2023)
ISSN : 2437-1114
www.aljest.org

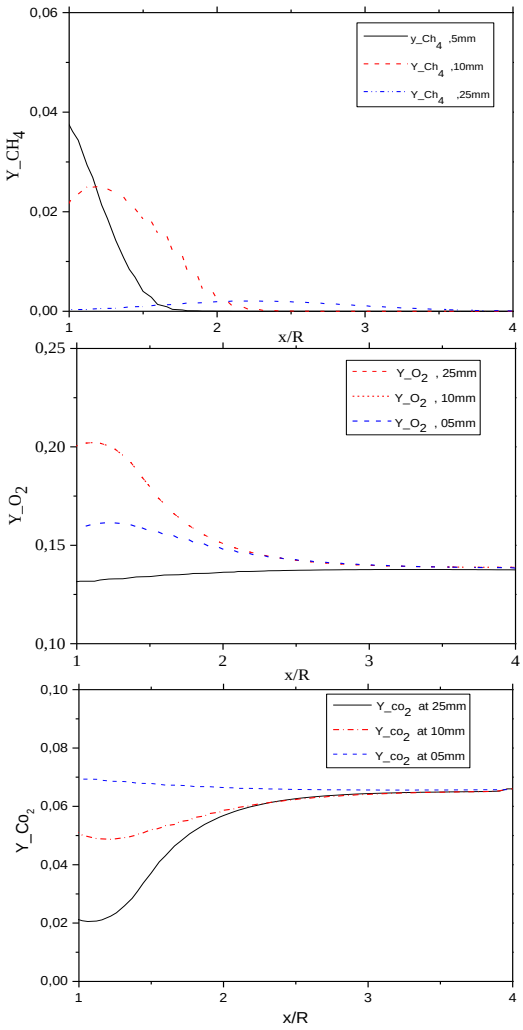

Figure 7. *CH_4, O_2 and CO_2 evolution at different section*

Figures 8, 9, 10 and 11 show the contours of oxidation and formation species in in the process of combustion. It has been seeing that the oxidation species represented by the O_2 and OH and the formation specie s or the product of the combustion represented by the CO_2 and H_2O. Figure 12 show the contours of the NO formation. It has been see that the mass fraction of NO distribution in the combustion chamber is according to the highest temperature distribution.

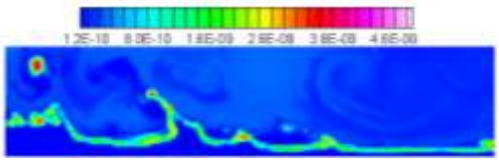

Figure 8. *Contour of the O_2 consomation evolution in the combustion process*

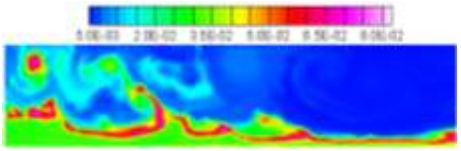

Figure 9. *Contour of H_2O evolution formation in the combustion process*

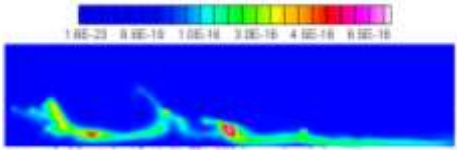

Figure 10. *Contour of CO_2 in the combustion chamber*

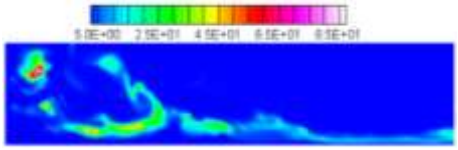

Figure 11. *Contour of OH in the combustion process*

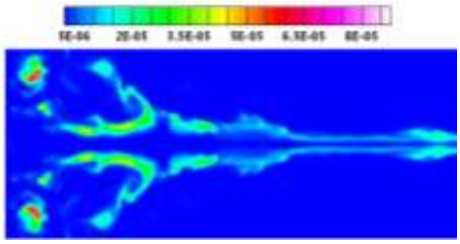

Figure 12. *Contours of NO Mass Fraction: Thermal NOx Formation*

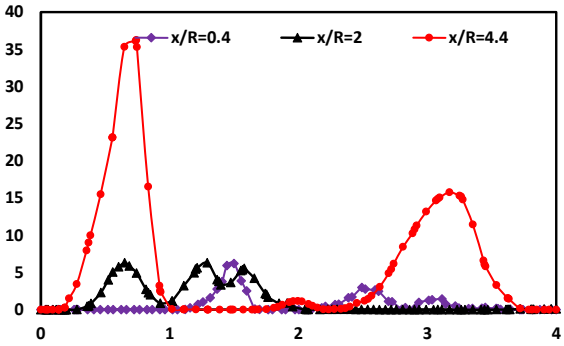

Figure 13*. Profiles of NO ppm: Prompt NOx Formation*

Figure13 Shows the variation of NO mass fraction at different section in the axial direction of the combustion chamber .In this chart we can see that at lowest value of achieved NO mass fraction is located at the lowest values of temperature. The NO

mass fraction increases respectively in highest value of temperature because it is a burned zone in combustion chamber.

IV. Conclusion

In this numerical investigation of combustion chamber shows following findings: the formations of NOx located on the high temperature. Giving less NO emission as less temperature in the combustion chamber.

For methane as fuel and with initial atmospheric conditions, the theoretical flame temperature produced by the flame with a fast combustion reaction is 2300 K. The predicted maximum flame temperature is 1800 K of the combustion products compares well with the theoretical adiabatic flame temperature. Temperature profiles shows increment at reaction zone due to burning of air-methane mixture and decrement in temperature downstream of dilution holes because more and more air will enter in combustion chamber to dilute the combustion mixture along center line . Specie namely NO is increasing and achieving peak point at reaction zone because they are products of combustion along centerline.

V. References

1. Selle, L.; Lartigue, G.; Poinsot, T.; Koch, R. K.; Schildmacher, U.; Krebs, W.; Kaufman, P.; Veynante, D. Compressible large eddy simulation of turbulent combustion in complex geometry on unstructured meshes. *Combustion and Flame* 137 (2004) 489-505.
2. Claypoleet, T. C.; Syred, N. The effect of swirl burner aerodynamics on NOx formation. *Proc. Combust. Institute.* 18 (1981) 81-89.
3. Magnussen, B. F.; Hjertager, B. H. On mathematical models of turbulent combustion with special emphasis on soot formation and combustion. *Proceedings of the Combustion Institute.* 16 (1976) 719-729.
4. Roux, S.; Lartigue, G.; Poinsot, T.; Meier, U.; Berat, C. Studies of mean and unsteady flow in a swirled combustor using experiments. Acoustic Analysis and Large Eddy Simulations. *Combustion and Flame* 141 (2005) 40-54.
5. Lalmi, D.; Hadef, R. Evaluation of the statistical approach for the simulation of a swirling turbulent flow. *American Journal of Mechanical and Engineering* AJME, Vol. 03, N°3A (2015) 27-31.
6. Merkle, K.; Haessler, H.; Büchner, H.; Zarzalis, N. Effect of CO and counter-swirl on the isothermal flow and mixture field of an airblast atomizer nozzle. *International Journal of Heat and Fluid Flow* 24 (2003) 529-537.
7. Lalmi, D.; Hadef, R. Evaluation of the Performance of two Turbulent Models in the prediction of a swirling flow. *International Journal of Mechanics and Energy* (IJME) Vol. 3, Issue 1, (2015), ISSN: 2286-584
8. Lalmi, D.; Hadef, R. Numerical simulation of CO and counter swirls on the isothermal flow and mixture field in a combustion chamber. *Advances and Applications in Fluid Mechanics* AAFM, Vol.18, issue 2 (October 2015) 199-212.
9. Syred, N.; Beer, J. M. Combustion in swirling flows: a review. *Combustion and Flame* 23/2 (1974) 143-201. http://dx.doi.org/10.1016/0010-2180(74)90057-1
10. Pierce, C. D.; Moin, P. Large eddy simulation of a confined coaxial jet with swirl and heat release. *American Institute of Aeronautics and Astronautics Paper* (1998) 2892.
11. Pierce, C. D.; Moin, P. Method for generating equilibrium swirling in flow conditions. *American Institute of Aeronautics and Astronautics* 36/7 (1998)1325-327. http://dx.doi.org/10.2514/3.13970
12. Lalmi, D.; Hadef, R. Numerical simulation of co and counter swirls on the isothermal flow and mixture field in a combustion chamber. *Advances and Applications in Fluid Mechanics* 18/2 (2015) 199. http://dx.doi.org/10.2514/6.1998-2892
13. Merkle, K.; Haessler, H.; Büchner, H.; Zarzalis, N. Effect of CO and counter swirl on the isothermal flow and mixture field of an airblast atomizer nozzle. *International Journal of Heat and Fluid Flow* 24/4 (2003) 529-537. http://dx.doi.org/10.1016/S0142-727X(03)00047-X.
14. Zhiyin, Y. Large-eddy simulation: Past, present and the future. *Chinese journal of Aeronautics* 28/1 (2015) 11-24. http://dx.doi.org/10.1016/j.cja.2014.12.007
15. Nickolaus, D. A.; Smith, C. E. Analysis of highly swirled, turbulent flows in dump combustor with exit contraction. *The American Society Of Mechanical Engineers Paper* N° GT2005-68160 (2005) 97-110. http://dx.doi.org/10.1115/GT2005-68160
16. McIlwain, S.; Pollard, A. Large eddy simulation of the effects of mild swirl on the near field of a round free jet. *Physics of Fluids* 14/2 (2002) 653-661. http://dx.doi.org/10.1063/1.1430734
17. Kumar, R.; Sood, S.; Sheikholeslami, M.; Shehzad, S. A. Nonlinear thermal radiation and cubic autocatalysis chemical reaction effects on the flow of stretched nanofluid under rotational oscillations. *Journal of Colloid and Interface Science* 505 (2017) 253-265. https://doi.org/10.1016/j.jcis.2017.05.083
18. Kumar, R.; Sood, S. Combined influence of fluctuations in the temperature and stretching velocity of the sheet on MHD flow of Cu-water nanofluid through rotating porous medium with cubic auto-catalysis chemical reaction. *Journal of Molecular Liquids* 237 (2017) 347-360. http://dx.doi.org/10.1016/j.molliq.2017.04.054
19. Manoj K. T.; Rajsekhar, P. Numerical analysis of natural convection in a triangular cavity with different configurations of hot wall. *International Journal of Heat and Technology* Vol. 35, No. 1, (March 2017) 11-18. DOI: 10.18280/ijht.350102.
20. Zakaria, M.; Aouissi, M.; Toufik, B. A Numerical study of swirl effects on the flow and flame dynamics in a lean premixed combustor. *International Journal of Heat and Technology* vol.34/2 (June 2016) 227-235. DOI: 10.18280/ijht.340211
21. Messaoud, H.; Bachir, M.; Djamel, S. Numerical study of mixed convection and flow pattern in various across-shape concave enclosures. *International Journal of Heat and Technology* 35 (2017) 567-575.
22. Tomczak, H. J.; Benelli, G.; Carrai, L.; Cecchini, D. Investigation of a gas turbine combustion system fired with mixtures of natural gas and hydrogen. *IFRF Combustion Journal*, (2002) 1-19.
23. Furuhata, T.; Amano, S.; Yotoriyama, K.; Arai, M. Development of can-type low NOx combustor for micro gas turbine (fundamental characteristics in a primary combustion zone with upward swirl). *Fuel Journal* 86(15), 2463-2474.

24. Benini, E.; Pandolfo, S.; Zoppellari, S. (2009). Reduction of NO emissions in a turbojet combustor by direct water/steam injection: Numerical and experimental assessment. *Applied Thermal Engineering* 29/17-18, (2007) 3506-3510.
25. Jaafar, M. M.; Jusoff, K.; Osman, M. S.; Ishak, M. S. A. Combustor aerodynamic using radial swirler. *International Journal of Physical Sciences* 6/13 (2011) 3091-3098.
26. Ghenai, C. Combustion of syngas fuel in gas turbine can combustor. *Advances in Mechanical Engineering* 2 (2010) 342357.

Acknowledgments

The authors thank the General Directorate of Scientific Research and Technological Development (DGRSDT) of Algeria for funding this research, which expressed its preliminary findings with this scientific article.

Please cite this Article as:
Lalmi D., Bellaouar A., Benali A., Hadef R., Analyse and NOx prediction in turbilent non-primexed swirling flame,***Algerian J. Env. Sc. Technology***, 9:2 (2023) 3070-3078**